PAPER

Multichannel-coupled compressed ultrafast photography

To cite this article: Jiali Yao *et al* 2020 *J. Opt.* **22** 085701

View the article online for updates and enhancements.

Multichannel-coupled compressed ultrafast photography

Jiali Yao[1,3], Dalong Qi[1,3], Chengshuai Yang[1], Fengyan Cao[1], Yilin He[1], Pengpeng Ding[1], Chengzhi Jin[1], Yunhua Yao[1], Tianqing Jia[1] , Zhenrong Sun[1] and Shian Zhang[1,2]

[1] State Key Laboratory of Precision Spectroscopy, School of Physics and Electronic Science, East China Normal University, Shanghai 200062, People's Republic of China
[2] Collaborative Innovation Center of Extreme Optics, Shanxi University, Taiyuan 030006, People's Republic of China

E-mail: tqjia@phy.ecnu.edu.cn and sazhang@phy.ecnu.edu.cn

Abstract

Compressed ultrafast photography (CUP) is currently the fastest receive-only ultrafast imaging technique with snapshot. CUP can capture non-repetitive transient events through three-dimensional (3D) image reconstruction based on a compressed sensing (CS) algorithm. However, CUP is a lossy imaging technique via image encoding and decoding, so how to further improve the image reconstruction accuracy has always been a goal pursued by scientists. Here, we develop a novel design of multichannel-coupled CUP (i.e. MC-CUP) to improve the image reconstruction accuracy. MC-CUP can not only increase the sampling rate, but also keep the snapshot of CUP. To demonstrate the advantage of MC-CUP in the image reconstruction accuracy, we measure a spatially modulated picosecond laser pulse and a 3D stepped structure, and these experimental results confirm that MC-CUP can significantly improve the spatial and temporal resolutions compared to CUP. This study will further promote the practical applications of CUP in ultrafast imaging, especially for biomedical imaging with high spatial resolution.

Keywords: optical imaging, computational imaging, compressed sensing, ultrafast measurement

(Some figures may appear in colour only in the online journal)

1. Introduction

Recording dynamic scenes at high imaging speed (i.e. high-speed imaging) has been of great interest to scientists and photographers for more than a century. In early days, high-speed imaging could be used to record fast moving macroscopic objects, such as the movement of horses and the flight of supersonic bullets [1, 2]. Nowadays, it can also be used to explore various phenomena in microscopic world, such as the electronic motion in non-equilibrium materials [3]. Currently, charge-coupled devices (CCD) and complementary metal oxide semiconductors (CMOS) are usually used as the imaging devices, but their maximal imaging frame rate can only reach 10^7 frames per second (fps) due to the limitation of chip storage and electronic readout speeds [4], and so the faster nanosecond and even picosecond events cannot be captured. Pump-probe technique is widely used to capture ultrafast dynamic scenes by adjusting the time delay between the pump and probe beams [5–7], but the repeated measurements make this technique unable to study some important non-repetitive events, such as irreversible chemical reaction dynamics [8, 9], or shock waves in inertial confined fusion [10]. In order to overcome this technical problem, Gao *et al* developed a compressed ultrafast imaging (CUP) technique by combining compressed sensing (CS) with streak imaging in 2014 [11], which can capture non-repetitive transient events at the speed of 10^{11} fps. Moreover, CUP is a receive-only device with snapshot, which is highly beneficial for imaging a variety of luminescent objects and non-repetitive (or irreversible)

---

[3] These authors contributed equally to this work.

transient events. Therefore, it has become a powerful tool in the field of ultrafast imaging [12] and has been successfully applied in many scientific studies, such as capturing the flying photons [11, 13], recording a three-dimensional (3D) object [14], and measuring the spatiotemporal intensity of ultrashort laser [15, 16].

In CUP, a dynamic scene is captured by streak camera after random encoding, and finally a CS algorithm is used to recover the original dynamic scene. The experimental data are collected through one imaging channel, and therefore the finally measured dynamic scene will lose about half of the information in spatial domain due to pseudo-random binary encoding, that is, CUP is a kind of lossy imaging. In addition, the image reconstruction via the algorithms also have certain computational errors. All these factors will lead to the low imaging reconstruction accuracy, including both the spatial and temporal resolutions. To make up for these defects, various improved schemes have been proposed in recent years, such as spatial-strength constraint or augmented Lagrangian reconstruction algorithm [17, 18], optimizing codes for CUP [19], and lossless-encoding CUP [13]. Here, we propose a novel design of multichannel-coupled CUP (i.e. MC-CUP) technique. In MC-CUP, the dynamic scene is divided into multiple replicas in space, then each replica passes through a different random encoding region, and finally all these encoded replicas are sent to a streak camera for imaging. Here, MC-CUP can not only increase the sampling rate, but also keep the snapshot. Our theoretical analysis and experimental results prove that MC-CUP can achieve great improvement in both the spatial and temporal resolutions compared to CUP.

2. Basic principle

In CS's framework, for a target signal $u \in R^N$ with u containing k non-zero values, it is assumed that the number of linear measurements M is obtained by a measurement matrix A, the sampling process can be described by the following mathematical model as [20, 21]

$$b = Au, \qquad (1)$$

where A is a matrix of size $M \times N$, and $b \in R^M$ is the measurement value obtained by sampling. Generally, $k < M \ll N$. If the noisy observation signal $b = Au + e$ is known, the core problem of CS is to reconstruct the original sparse signal u based on b, that is, it is to solve an inverse problem. Here, the solution of inverse problem $\hat{u}$ (i.e. a restored signal) by minimizing an objective function $f(u)$, which can be written as [22–24]

$$\hat{u} = \arg\min_u \{f(u)\}, \qquad (2)$$

with

$$f(u) = \frac{1}{2} \|b - Au\|_2^2 + \lambda \Phi(u), \qquad (3)$$

where $\|.\|_2$ is the l_2 norm, λ is the regularization parameter, and $\Phi(u)$ is the regularization function.

However, what is M that can ensure the original signal being reconstructed without distortion? Previous studies have shown that M should satisfy such a relation of [25–27]

$$M \geqslant F \cdot \mu^2 \cdot k \cdot \ln N, \qquad (4)$$

where F is a constant, k is the number of non-zero elements of the original signal in the sparse domain, and μ is the coherence between measurement domain and sparse expression domain [27]. It can be seen from equation (4) that one can increase M or decrease μ in order to recover the original signal accurately. The error ε between the reconstructed signal $\hat{u}$ and the original signal u can be expressed as [20]

$$\varepsilon = \|u - \hat{u}\|_2 \leq C_r \cdot \left(\frac{M}{\log N} \right)^{-(1/p - 1/2)} \quad (0 < p < 1), \quad (5)$$

where C_r is a constant that is correlated with u. It can be seen from equation (5) that the larger M will yield the smaller ε.

In CUP, the dynamic scene $I(x, y, t)$ is first encoded with a pseudo-random binary pattern generated by a digital micromirror device (DMD), and then the encoded dynamic scene is sent into a streak camera for temporal shearing and spatiotemporal integration. This process can be mathematically formulated as [11]

$$E(x', y') = \text{TSC}I(x, y, t), \qquad (6)$$

where $E(x', y')$ is the observation image captured by the steak camera, C is a spatial encoding operator, S is a temporal shearing operator, and T is a spatiotemporal integration operator.

In our designed MC-CUP, the dynamic scene is divided into three replicas, and each replica is encoded by a different pseudo-random binary code, as shown in figure 1. In this case, the sampling process can be further written as

$$\begin{bmatrix} E_1(x', y') \\ E_2(x', y') \\ E_3(x', y') \end{bmatrix} = \begin{bmatrix} \text{TSC}_1 \\ \text{TSC}_2 \\ \text{TSC}_3 \end{bmatrix} I(x, y, t). \qquad (7)$$

Here, M is equal to 3. Based on equations (4) and (5), it is obvious that MC-CUP can effectively decrease the image reconstruction error ε, and therefore a higher image reconstruction accuracy can be obtained, which is mainly embodied by the higher spatial and temporal resolutions.

In the image reconstruction, a two-step iterative shrinkage/thresholding (TwIST) algorithm is used to solve equations (6) and (7) in reverse [28], and the regularization function $\Phi(I)$ is defined as the total variation (TV) of the dynamic scene, which encourages sparsity in the gradient domain and can be expressed as

$$\Phi_{TV}(I) = \sum_{k=0}^{N_t - 1} \sum_{i,j} \|D_{i,j} I_k\|_2 + \sum_{m=1}^{N_x} \sum_{i,j} \|D_{i,j} I_m\|_2$$
$$+ \sum_{n=1}^{N_y} \sum_{i,j} \|D_{i,j} I_n\|_2. \qquad (8)$$
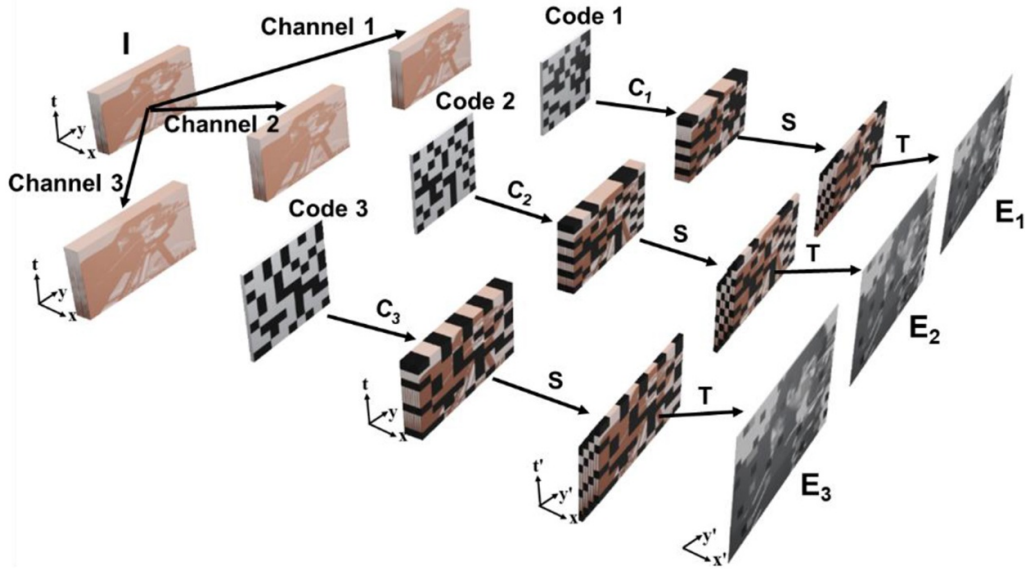
Figure 1. Schematic diagram of data acquisition for MC-CUP, where t, t': time; x, y: spatial coordinates at the object; x', y': spatial coordinates at the streak camera; $C_i(i = 1,2,3)$: spatial encoding operator; S: temporal shearing operator; and T: spatiotemporal integration operator.

Here, m, n, and k represent the discrete indices of I in the x, y, and t directions and I_m, I_n, I_k respectively denote the 2D lattices along the dimensions m, n, k. N_x, N_y, and N_t correspond to the size of the discretized form of I. $D_{i,j}$ are horizontal and vertical first order local difference operators at pixel (i, j) on a two-dimensional lattice. Meanwhile, the regularization parameter λ can be adjusted to guide the reconstruction results with almost identical physical reality. In addition, a flow chart of the TwIST algorithm employed for image reconstruction is shown in figure 2. A two-step iteration is operated to obtain $I_{i+1}(m, n, k)$ through the results from the previous two iterations, where i denotes to the number of iteration, and it enables the TwIST algorithm to have a fast convergence speed and high accuracy of solution.

3. Experimental setup

The experimental arrangement of MC-CUP is shown in figure 3(a). A dynamic scene is individually imaged on an optical glass plate covered with a pseudo-random binary pattern via three side-by-side imaging systems, that is, the dynamic scene is splitted into three replicas. Each imaging system contains two 8 mm diameter lenses with the focal lengths of 10 and 30 mm, respectively. The three encoded replicas are sent into a streak camera (Hamamatsu, C7700) for measurement via a 4 f imaging system. This imaging system is composed of two 25.4-mm-diameter lenses with the focal lengths of 200 and 150 mm, respectively. Here, the lens sizes and focal lengths in these imaging systems are properly designed to make the whole system more compact and make full use of CMOS pixels in the streak camera. As shown in figure 3(b), the three replicas pass through the entrance slit of the streak camera in parallel in the horizontal direction, where the slit is fully opened for imaging, and the three captured images

on CMOS are very close in the horizontal space, but do not overlap. Additionally, the encoder in our MC-CUP is different from DMD in conventional CUP, here it is a kind of transmissive encoding device, where a piece of silver film with a length of 5 cm, a width of 1.5 cm and a thickness of 100 nm is randomly hollowed out about 50% in space, and then the fabricated silver film is coated on a k9 optical glass plate for fixing. The designed silver film can block a portion of photons, and the remaining photons pass through the optical glass plate, thus the dynamic scene is spatially encoded in the intensity.

4. Results and discussion

4.1. Improvement in spatial resolution

To demonstrate that MC-CUP can improve the spatial resolution compared to CUP, we measure the spatiotemporal evolution of an E-shaped laser pulse with our MC-CUP system, as shown in figure 4(a). A mode-locked Ti:sapphire laser amplifier is used to generate a laser pulse with the temporal width of about 200 ps, central wavelength of 800 nm and repetition rate of 100 Hz. The output laser pulse is expanded to illuminate a hollow letter E fabricated in a black nylon plate. The photons within the letter E can pass through the nylon plate, while the ones outside are blocked. The E-shaped laser pulse is projected onto a white thin paper, and a small portion of photons can pass through it. Thus, the spatiotemporal evolution of the E-shaped laser pulse on the white paper can be measured using our MC-CUP system.

The reconstructed images in our MC-CUP experiment are shown in figure 4(c). The spatial structure of letter E can be clearly demonstrated, and its entire evolution process from appearance to disappearance can also be well observed. The reconstructed images for CUP with one imaging channel are
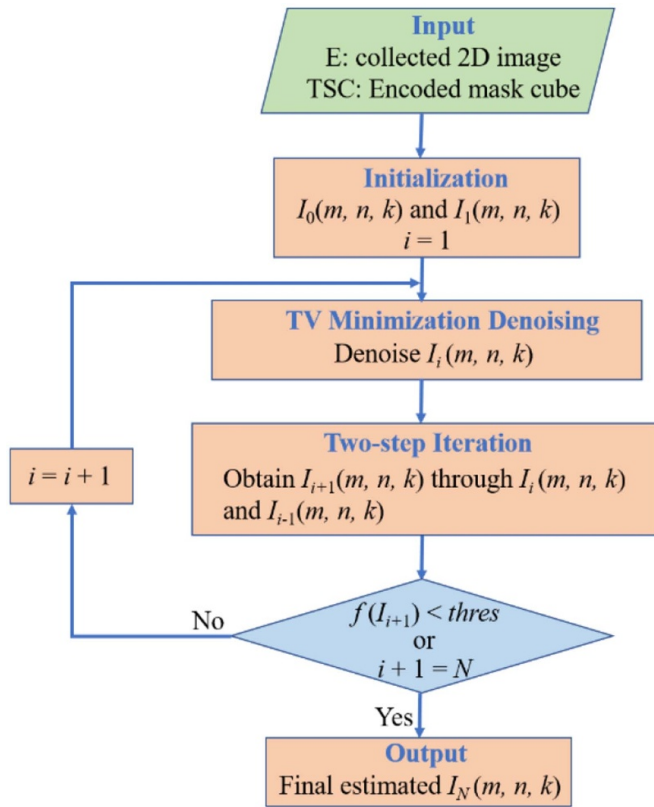
Figure 2. A flow chart of the TwIST algorithm.

Figure 3. (a) Schematic diagram of MC-CUP. (b) Detailed illustration of the streak camera, MCP: micro-channel plate.

also given, as shown in figure 4(b). The spatial profile of letter E is not fully displayed, especially at the highest intensity with the time of 280 ps. By comparison, it can be found that the reconstructed letter E by MC-CUP has the sharper edge and the clearer profile than that by CUP. To further illustrate the improvement in the spatial resolution for MC-CUP, the intensities of the E-shaped laser pulse at the time point of 280 ps in figures 4(b) and (c) are integrated along the horizontal direction, and the calculated results are given in figure 4(d). Compared to CUP, MC-CUP has a higher signal-noise ratio (SNR) for the second and third peaks, corresponding to the middle and bottom horizontal lines of letter E. Additionally, the intensity evolutions of the E-shaped laser pulses in figures 4(b) and (c) are also extracted to further compared, as shown in figure 4(e). The directly measured result by the streak camera is taken as a reference. Different from the usage of MC-CUP or CUP, here the entrance slit of the streak camera is closed to a few microns, which is the commonly used method of streak camera [29]. Both MC-CUP and CUP can demonstrate the temporal evolution behavior of the E-shaped laser pulse well, but MC-CUP has a slightly higher detection accuracy.

4.2. Improvement in temporal resolution

In 3D imaging, the time of flight (ToF) detection is a common method [14, 30, 31]. A laser pulse is used to illuminate a 3D object, an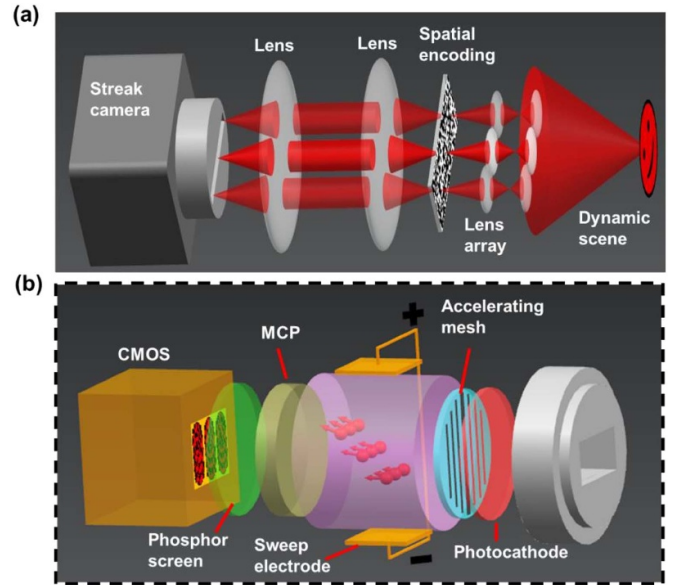d the photons scattered from the surface of the object are received by a detector. Thus, the depth information of the object can be obtained by measuring the round-trip ToF signal of the laser pulse, and it is given by

$$z = c \cdot t_{ToF}/2, \qquad (9)$$

where c is the speed of light. One can see from equation (9) that the temporal resolution of the detector can be characterized by measuring the depth resolution, and the higher the spatial resolution is, the higher the temporal resolution can achieve. Here, we employ this method to compare the temporal resolutions of MC-CUP and CUP.

To measure the depth resolutions of MC-CUP and CUP, a 3D stepped structure with alternating lengths is fabricated using white nylon through 3D printing, as shown in figure 5(a). This stepped sample has 6 steps, and each step has a width of 3 mm and a height of 3 mm. A 50 fs laser pulse illuminates the 3D stepped structure after passing through an engineered diffuser (ED). The MC-CUP system is placed in the vertical direction of the stepped sample surface and collects the backscattered photons from the surface, as shown in figure 5(b). Similarly, the reconstructed images for MC-CUP and CUP are presented, as shown in figures 5(c) and (d). For comparison, only three representative images at the time points of 52, 72 and 92 ps are given. In each image, four steps can be observed by CUP, while only three steps by MC-CUP. Thus, the depth resolutions of MC-CUP and CUP are 6 and 9 mm, respectively. Based on equation (9), the temporal resolutions for MC-CUP and CUP can be calculated as 40 and 60 ps, respectively. Therefore, MC-CUP has the higher temporal resolution than CUP. Obviously, MC-CUP can provide an effective method to further improve the temporal resolution.
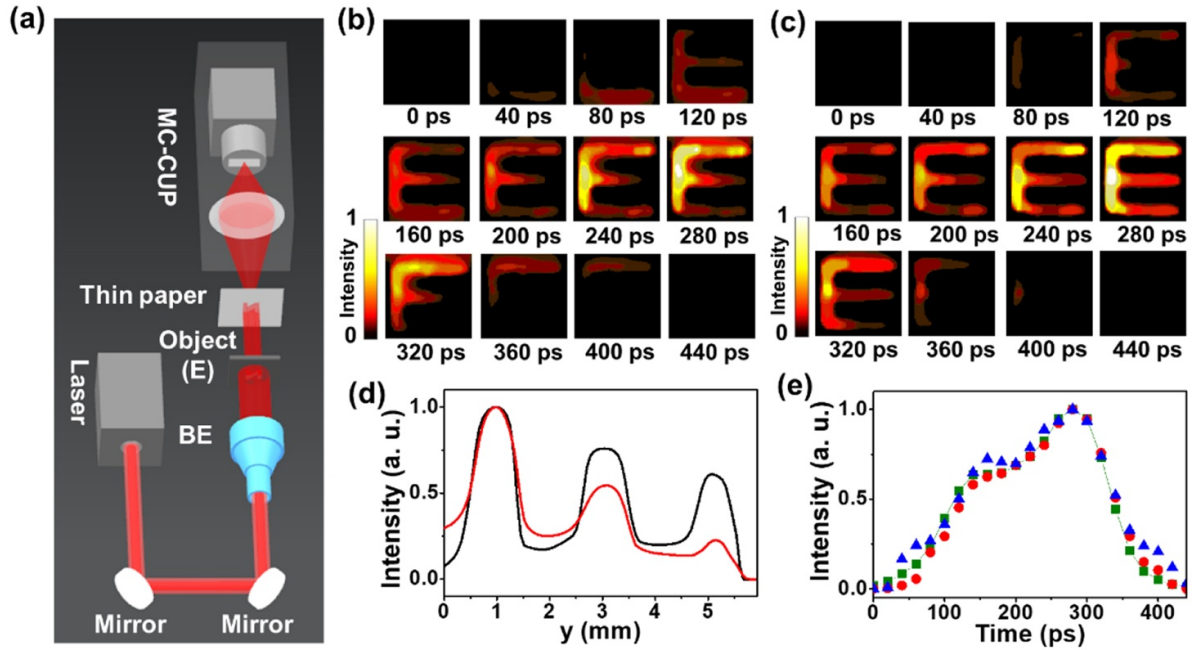
Figure 4. (a) Experimental setup for the spatiotemporal measurement of E-shaped laser pulse, BE: beam expander. (b), (c) Reconstructed images by CUP and MC-CUP. (d) Integrated intensities along horizontal direction for the reconstructed images with the time of 280 ps in (b) (red line) and (c) (black line). (e) Extracted intensities from (b) (blue triangles) and (c) (red circles), together with the measured result by streak camera (green squares).
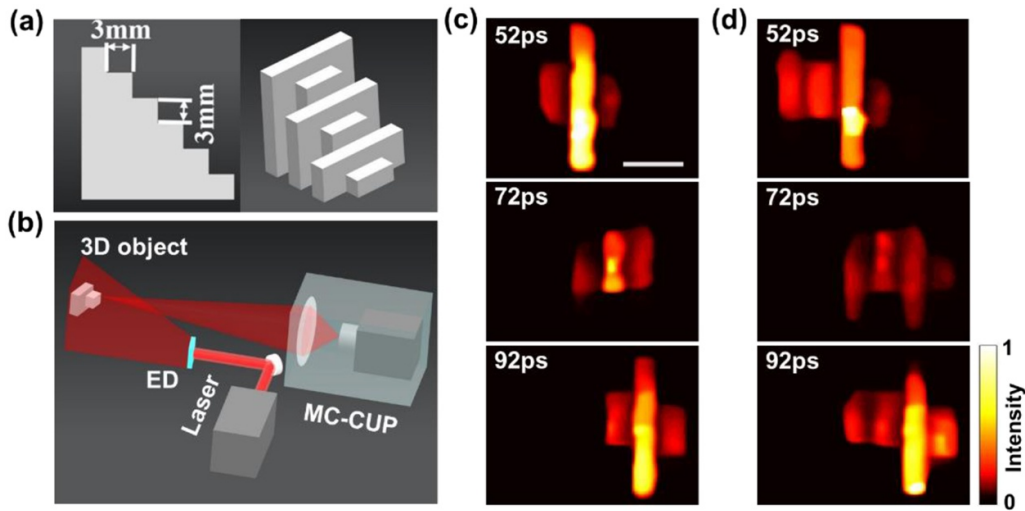
Figure 5. (a) Side view and photograph of a 3D stepped sample. (b) Experimental setup for the depth resolution measurement by illuminating the 3D stepped sample. (c), (d) Reconstructed images at the time points of 52, 72 and 92 ps by MC-CUP and CUP, scale bar: 9 mm.

4.3. Technical limitations in applications

As shown above, MC-CUP has the higher spatial and temporal resolutions than CUP. In theory, the more imaging channels the MC-CUP has, the better reconstruction results it can achieve, as shown in equation (5). However, the number of the imaging channels still needs to be limited. Firstly, the more imaging channels will result in the fewer CMOS pixels occupied in each channel, which will seriously affect the spatial resolution. Secondly, these imaging channels need to be arranged in a row due to the limitation of the entrance slit and the vertical

deflection in the streak camera, as shown in figure 3(b), thus if too many imaging channels are employed, those imaging channels on the side will cause the image distortion. To couple these images on CMOS in the image reconstruction well, all the images are required to be highly consistent in the spatial information.

In MC-CUP, the light flux in each imaging channel will be greatly reduced compared to the single channel of CUP. To ensure that each imaging channel can obtain clear image on CMOS, the dynamic scene needs to have high radiation or reflection intensity. In particular, the photocathode of the

streak camera needs a certain laser excitation threshold to produce photoelectrons. Therefore, MC-CUP is not suitable for the measurement of weak dynamic scene signal. Actually, CUP can only measure the stronger signals because of the limitation of high data compression ratio, let alone MC-CUP.

Additionally, the TwIST algorithm based on TV regularization only exploited image sparsity in the gradient domain, which makes it effective but less adjustable to provide high-quality reconstructed images. Fortunately, some plug-and-play algorithms have shown to be higher flexibility and better performance by incorporating multiple priors of various advanced denoisers for image recovery [32, 33]. For example, the plug-and-play regularization (PPR) algorithm employed depth prior of the image based on a fast and flexible denoising convolutional neural network (FFDNet) denoiser [32], and the constrained phase retrieval (ConPR) algorithm used non-local similarity and 3D transform sparsity of the underlying image based on a block matching and 3D filtering (BM3D) denoiser [33]. It can be prospected that, by introducing these novel reconstruction algorithms, MC-CUP is expected to be widely applied in the field of ultrafast imaging.

5. Conclusions

In summary, we have developed MC-CUP to solve the problem of low image reconstruction accuracy in CUP. Compared to CUP, MC-CUP can further improve the spatial and temporal resolutions by increasing the sampling rate, it is highly desired for the measurement of transient events with complex spatial structure. Moreover, MC-CUP greatly improves the performance of CUP, which is very helpful to promote the applications of CUP. In future studies, MC-CUP can be further combined with a microscope or telescope, which has potential applications in biological imaging and astrophysics.

Acknowledgments

ORCID iDs

Tianqing Jia https://orcid.org/0000-0002-7497-1921
Shian Zhang https://orcid.org/0000-0003-3168-4962

References

[1] Munn O D and Beach A E 1878 A horse's motion scientifically determined *Sci. Am.* **39** 241
[2] Mach E and Salcher P 1887 Photographische Fixirung der durch Projectile in der Luft eingeleiteten Vorgänge *Ann. Phys.* **268** 277
[3] Hu S X and Collins L A 2006 Attosecond pump probe: exploring ultrafast electron motion inside an atom *Phys. Rev. Lett.* **96** 073004
[4] Kondo Y *et al* 2012 Development of 'HyperVision HPV-X' high-speed video camera *Shimadzu Rev.* **69** 285
[5] Nobel Media AB 2020. The Nobel Prize in Chemistry 1999 (https://www.nobelprize.org/prizes/chemistry/1999/summary/) (Accessed: 4 March 2020)
[6] Siwick B J, Dwyer J R, Jordan R E and Miller R D 2003 An atomic-level view of melting using femtosecond electron diffraction *Science* **302** 1382
[7] Hockett P, Bisgaard C Z, Clarkin O J and Stolow A 2011 Time-resolved imaging of purely valence-electron dynamics during a chemical reaction *Nat. Phys.* **7** 612
[8] Park S T, Flannigan D J and Zewail A H 2011 Irreversible chemical reactions visualized in space and time with 4D electron microscopy *J. Am. Chem. Soc.* **133** 1730
[9] Yang J *et al* 2018 Imaging CF_3I conical intersection and photodissociation dynamics with ultrafast electron diffraction *Science* **361** 64
[10] Craxton R S *et al* 2015 Direct-drive inertial confinement fusion: a review *Phys. Plasmas* **22** 110501
[11] Gao L, Liang J, Li C and Wang L V 2014 Single-shot compressed ultrafast photography at one hundred billion frames per second *Nature* **516** 74
[12] Qi D *et al* 2020 Single-shot compressed ultrafast photography: a review *Adv. Photonics* **2** 014003
[13] Liang J, Ma C, Zhu L, Chen Y, Gao L and Wang L V 2017 Single-shot real-time video recording of a photonic Mach cone induced by a scattered light pulse *Sci. Adv.* **3** e1601814
[14] Liang J, Gao L, Hai P, Li C and Wang L V 2015 Encrypted three-dimensional dynamic imaging using snapshot time-of-fight compressed ultrafast photography *Sci. Rep.* **5** 15504
[15] Liang J, Zhu L and Wang L V 2018 Single-shot real-time femtosecond imaging of temporal focusing *Light Sci. Appl.* **7** 42
[16] Cao F *et al* 2019 Single-shot spatiotemporal intensity measurement of picosecond laser pulses with compressed ultrafast photography *Opt. Lasers Eng.* **116** 89
[17] Zhu L, Chen Y, Liang J, Xu Q, Gao L, Ma C and Wang L V 2016 Space- and intensity-constrained reconstruction for compressed ultrafast photography *Optica* **3** 694
[18] Yang C, Qi D, Cao F, He Y, Wang X, Wen W, Tian J, Jia T, Sun Z and Zhang S 2019 Improving the image reconstruction quality of compressed ultrafast photography via an augmented Lagrangian algorithm *J. Opt.* **21** 035703
[19] Yang C *et al* 2018 Optimizing codes for compressed ultrafast photography by genetic algorithm *Optica* **5** 147
[20] Candès E J and Tao T 2006 Near-optimal signal recovery from random projections: universal encoding strategies? *IEEE Trans. Inf. Theory* **52** 5406
[21] He Z, Ogawa T and Haseyama M 2010 The simplest measurement matrix for compressed sensing of natural images *Proc. 17th IEEE Int. Conf. Image Process.* p 4301
[22] Wright S J, Nowak R D and Figueiredo M A 2009 Sparse reconstruction by separable approximation *IEEE Trans. Signal Process.* **57** 2479
[23] Figueiredo M A, Nowak R D and Wright S J 2007 Gradient projection for sparse reconstruction: application to compressed sensing and other inverse problems *IEEE J. Sel. Top. Signal Process.* **1** 586
[24] Elad M, Matalon B and Zibulevsky M 2007 Coordinate and subspace optimization methods for linear least squares with non-quadratic regularization *Appl. Comput. Harmon. Anal.* **23** 346
[25] Candès E J, Romberg J K and Tao T 2006 Stable signal recovery from incomplete and inaccurate measurements *Commun. Pure. Appl. Math.* **59** 1207

[26] Candès E J and Plan Y 2011 A probabilistic and RIPless theory of compressed sensing *IEEE Trans. Inf. Theory* **57** 7235

[27] Candès E J and Wakin M B 2008 An introduction to compressive sampling *IEEE Signal Process. Mag.* **25** 21

[28] Bioucas-Dias J and Figueiredo M 2007 A new TwIST: two step iterative shrinkage/thresholding algorithms for image restoration *IEEE Trans. Image Process.* **16** 2992

[29] Guide to streak cameras (https://wwww.hamamatsu.com/ resources/pdf/sys/SHSS0006E_STREAK.pdf) (Accessed: 26 May 2020)

[30] Hansard M, Lee S, Choi O and Horaud R 2012 *Time-of-Flight Cameras: Principles Methods and Applications* (Berlin: Springer)

[31] Oggier T *et al* 2004 An all-solid-state optical range camera for 3D real-time imaging with sub-centimeter depth resolution (SwissRanger) *Proc. SPIE* **5249** 534

[32] Shi B, Lian Q and Fan X 2019 PPR: plug-and-play regularization model for solving nonlinear imaging inverse problems *Signal Process.* **162** 83

[33] Shi B, Lian Q, Huang X and An N 2018 Constrained phase retrieval: when alternating projection meets regularization *J. Opt. Soc. Am.* B **35** 1271